Probing material nonlinearity at various depths by time reversal mirrors

Cedric Payan, T. J. Ulrich, P. Y. Le Bas, M. Griffa, P. Schuetz, M. C. Remillieux, T. A. Saleh

Probing material nonlinearity at various depths by time reversal mirrors

C. Payan[1], T.J. Ulrich[2], P.Y. Le Bas[2], M. Griffa[3], P. Schuetz[3], M.C. Remillieux[2], T.A. Saleh[4]

[1]Aix Marseille Université, LMA UPR CNRS 7051, 31 chemin Joseph Aiguier,
13402 Marseille, France
[2]Los Alamos National Laboratory, EES-17, Los Alamos, NM 87545, USA
[3]Swiss Federal Laboratories for Materials Science and Technology (EMPA), Überlandstrasse 129,
8600 Dübendorf, Switzerland
[4]Los Alamos National Laboratory, MST-16, Los Alamos, NM 87545, USA

Abstract

In this letter, the time reversal mirror is used to focus elastic energy at a prescribed location and to analyze the amplitude dependence of the focus signal, thus providing the nonlinearity of the medium. By varying the frequency content of the focused waveforms, the technique can be used to probe the surface, by penetrating to a depth defined by the wavelength of the focused waves. The validity of this concept is shown in the presence of gradual and distributed damage in concrete by comparing actual results with a reference nonlinear measurement and X ray tomography images.

The principle of time reversal acoustics is based on a simple idea. In any medium, send a pulse from a source. That pulse propagates into the medium. The pulse is eventually reflected many times at the boundaries and by other scatterers. The resulting signal is recorded at a defined location by a receiver. If the recorded signal is time reversed and sent back from the receiver, the wave will play this propagation history backward (as a movie played backward). The wave energy will focus at the precise source location, at a given time (namely the focal time). Thanks to the reciprocity principle [1], the same scenario can be achieved even if the time reversed signal is sent back from the initial source. In this case, the focus will occur at the receiver location. While this is true with a single emitter, using multiple emitters allows for a proportionately higher amplitude to be obtained at the focal time.

This physical principle has been under study for many years and has been largely developed by Fink [2] with most of the applications in liquids or biological tissues for the medical field. Applications to the field of nonlinear elasticity in solids were developed with the goal of using the high energy focus to extract some nonlinear properties of solids. It has been successfully applied to locate and image cracks in a metal component [3], to evaluate the quality of diffusion bonds [4], and to probe the interior of a solid [5]. To probe the nonlinearity of the medium with varying amplitude time reversal experiments, so far most of the studies have employed the harmonic content [3] or a scaled subtraction method [6,7]. However, these methods are dedicated to locate or size a single or multiple nonlinear scatterer embedded in a linear medium. They proved very efficient for nonlinear source localization. Here we explore the applicability to volumetrically distributed cracks in a nonlinear material.

The aim of this letter is to propose a physics-based method to measure the nonlinearity of the medium and to evaluate the nonlinearity at various depths. To provide a reliable nonlinear parameter, we make use of concrete samples whose nonlinear elastic behavior was assessed by a quantitative Nonlinear Resonant Ultrasound Spectroscopy (NRUS) measurement. The same samples are in this work also inspected by X-ray tomography to search for evidence of damage, usually considered as the source of the nonlinear behavior [8]. The reader is invited to refer to [8] for details about samples and NRUS results. To probe the nonlinearity at various depths, the frequency content of the transmitted signals is modified. It results in a variable focal spot size which depends on the wavelength.

The experiments are conducted on four concrete samples of size $10\times10\times6$ cm^3. The first sample remains undamaged while the others are thermally damaged at 120, 250 and 400°C, respectively. A plexiglass sample with the same geometry is also used as a linear elastic reference sample. The experimental protocol is based on reciprocal time reversal (abbreviated “TR” hereafter). The sample is placed onto a reverberant cavity which is a simple aluminum block with 8 piezoelectric discs (emitters) bonded to the surface at various locations. This cavity allows multiple reflections to occur, delaying the information available over time. It has been shown that both multiple reflections at the boundaries and multiple scattering improve the efficiency of the time reversal process [9]. A laser vibrometer records the out-of-plane particle velocity at the top of the sample. An 8-channel 14-bit

generator/digitizer system is used for signal generation and acquisition. The generator is connected to an 8-channel amplifier, which drives the emitters up to a 100Vpp voltage. A computer controls the TR experiments and allows moving the sample with a synchronized motion controller.

Five frequencies (f=100, 150, 200, 250 and 300kHz) corresponding to various wavelengths are selected. Note that the wavelength varies as a function of speed of sound c as $\lambda=c/f$. The size of the focus, i.e., the penetration depth, is known to correspond to $\lambda/2$ [1,6]. Over the full set of samples and frequencies, the wavelengths range from 9mm to 48mm. A chirp signal (sinusoid with frequency varying in a given range) with a 50kHz bandwidth is sent to one emitter. The signal is recorded by the laser vibrometer, cross-correlated with the initial chirp signal (this operation allows obtaining the impulse response of the sample in the selected frequency range) and recorded by the system. The same chirp is emitted from another emitter and the corresponding propagated signal is recorded as well. This process is executed for each channel. When the 8 impulse responses are recorded, a signal containing 4 successive amplitudes (scaled by 1, 0.9, 0.8 and 0.7 respectively) is built for each channel. All of them are then time reversed and sent back from their initial emitters simultaneously. The laser then records the four resulting focused waves, repeated each 50ms to average 64 times. This process is performed for 4 increasing voltages (12.5, 25, 50 and 100Vpp respectively) producing a total of 16 amplitudes. The full protocol is repeated at 2 other locations on the sample, 2cm away from each other's, in order to average the nonlinearity over the surface.

In materials such as rocks and concrete, so called nonlinear mesoscopic elastic materials [10], several nonlinear and non-equilibrium phenomena occur. The phenomenon of interest in this work is related to the material softening subjected to high strain waves ($\sim 10^{-6}$), also called fast dynamics. Figure 1(a) shows an example of a recorded retro focal time series zoomed at focal time. It is noticeable [refer to the dotted circles] that the zero crossing occurs at the same time for each amplitude in the linear Plexiglas sample while a time delay is clearly visible in the 400°C sample. The focal time appears more delayed, due to the decreasing speed of sound with increasing amplitude, a signature of the material softening. This time shift refers to the relative resonance frequency shift measured in NRUS experiments [8]. The softening of the material is evaluated as the relative velocity change $\Delta c/c_0$ with c_0 being the low amplitude speed of sound. The time delay Δt between signals is estimated by the cross-correlation of the low amplitude signal with higher amplitudes ones, similarly to the methods used by Rivière *et al.* [11] and Tournat *et al*. [12], for assessing nonlinearity. For more accuracy, the maximum position of the cross correlation is obtained by fitting the peak region with an oversampled second order polynomial function. The delay measured for the 400°C sample [Fig.1(a)] is 7ns for the highest amplitude. Over all measurements, the delay ranges from 20ps. to 140 ns.

As most of the energy is concentrated into a $\lambda/2$ region, the hypothesis is that the focused waves reach the softening nonlinear regime [13] only in this region. Assuming in first approximation the retro-focused wave field as a standing wave in a volume extended in depth for a length of $\lambda/2$, the relative velocity change can be approximated as $\Delta c/c_0 = - \Delta t/t_0 \approx - 2f \Delta t$, where f is the central

frequency of the chirp source signal and t_0 the time of flight for a λ/2 path. Similar to NRUS experiments [8], the nonlinearity parameter α is extracted from the slope of the relative velocity change versus the strain amplitude $\Delta c/c_0 = \alpha\ \Delta\varepsilon$ [solid lines Fig.1(b)]. The relative velocity change is averaged over the three measurements points at the surface of the sample. As an approximation, the strain amplitude is evaluated as $\Delta\varepsilon_{zz} \approx \Delta v_{zz}/c_0$ where Δv_{zz} is the out-of-plane particle velocity amplitude recorded by the laser. Due to the dispersive nature of concrete, the speed of sound c_0 is measured by time of flight for each frequency. Figure 1(b) shows results at 150 kHz. As expected, the Plexiglas sample is less nonlinear than concrete ones and the nonlinearity increases with thermal damage in the concrete samples.

Imperfections in the linear fit Fig. 1(b) are explained by experimental considerations associated with the coupling between nonlinearity and conditioning [14]. In each curve plotted in Fig. 1(b), considering a group of four points, the successive 4 amplitudes focused waves, averaged 64 times, make the material conditioned at the highest amplitude. Therefore, for the lower amplitudes, the material does not have time to entirely recover. Due to experimental conditions, the other groups of points are recorded about one minute later, leaving time to the material to recover. By considering only the highest amplitude signals at each voltage (suppressing the cited effect) the results are affected by less than 2%. However, as for NRUS, time delay is evaluated under fully conditioned conditions. It is also noticeable that in some cases Fig. 1(b), the fit could also apply with a quadratic function. Over the entire data set, there is no general trend allowing to draw a conclusion. However, this nonlinear trend can be explained by the strain estimation which relates more the effect of pressure components here. The complex interplay of compressional and shear components at the focus is not accounted, thus depending on the orientation of the microcracks into the focal spot, it is likely that the nonlinearity could answer more to shear than pressure waves or inversely. The full set of results is presented and discussed in the next section.

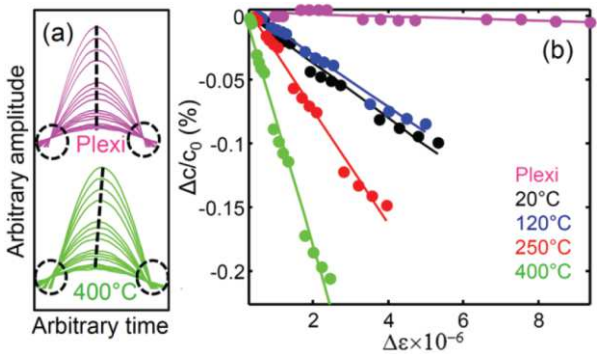

FIG. 1. (Color online) (a) Zoom at focal time for the linear plexiglass sample and the most damaged sample at 150kHz. For clarity, the time delay is magnified. (b) Relative velocity change at 150kHz for the full set of sample.

Fig.2 relates the full set of results and validations. Figure 2(a) shows the nonlinearity as a function of penetration depth for the full set of samples. The linear reference, i.e., the plexiglass sample, is one order of magnitude less nonlinear than the concrete. It provides the Signal-to-Noise Ratio (SNR) of this experiment. The SNR is more important in this measurement than for the NRUS measurement performed on the same samples [8]. Due to the homogeneity of thermal damage in concrete [15], the 20,120 and 250°C samples exhibit roughly constant nonlinearity. For the full set of concrete samples, the evolution of the average nonlinearity matches very well the reference NRUS measurements [See [8] and Fig. 2(c)]. The underestimation of the nonlinearity in the present study is due to the strain evaluation which is approximated by $\Delta\varepsilon_{zz}$ measured at the surface instead of the volumetric strain evaluated in [8]. Janssen et al. [6] have shown that the focal shape looks like a pear shape with a maximum volumetric stress at the surface. Considering the interaction zone as the whole focal spot, the average strain amplitude should be lower than the one measured at the surface. This leads to an overestimation of the strain amplitude, which tends to decrease the nonlinear parameter.

Figure 2(a) shows that the 400°C sample does not exhibit a constant nonlinearity with the depth of the material, with a clear increase of the nonlinearity in the near surface (~1cm). To understand this result, X-ray tomography measurements are performed on the reference concrete sample (20°C) and on the 400°C one. The details of such measurements are reported in the Supplementary Materials [15]. During thermal loading of concrete, the main damage (thus nonlinearity) source consists of debonding at the interface between the cement paste and the aggregates [8,16]. Figure 2(b) shows two vertical, digital cross-sections extracted from two X-ray tomographic datasets, one dataset for the reference sample at 20°C (top image), the other dataset for the sample thermally loaded at 400°C (bottom image). The arrows overlaid on top of the two images point to regions of potential debonding between the aggregate and the cement paste. Despite the low spatial resolution (about 100 μm) compared with the debonding size, it is clear from the two sample images that such regions of potential debonding are more frequent and much more widespread in the thermally loaded sample. A semi-quantitative, 2D image analysis of such regions is presented in the Supplementary Materials [15] and it confirms that the thermally loaded sample is characterized by aggregate-to-cement paste boundary regions with more debonding features. The bottom image in Fig. 2(b) clearly shows that the debonding runs all along the boundaries between a large aggregate and the surrounding cement paste. Signs of debonding with such a spatial extension are present in other parts of the sample. However, their concentration is larger within the first centimeter from the surface. This is due to aggregate segregation by size, occurring during mixing, leading to a higher number of large aggregates closer to the surface than in depth. Larger aggregates correspond to smaller inter-aggregate distances, which then leads to larger, localized thermal stresses in the cement paste, thus more frequent debonding [16]. In addition, debonding at the aggregate-cement paste interface is also driven by drying shrinkage, which occurs more easily closer to the surface [17], especially at elevated temperature such as 400°C.

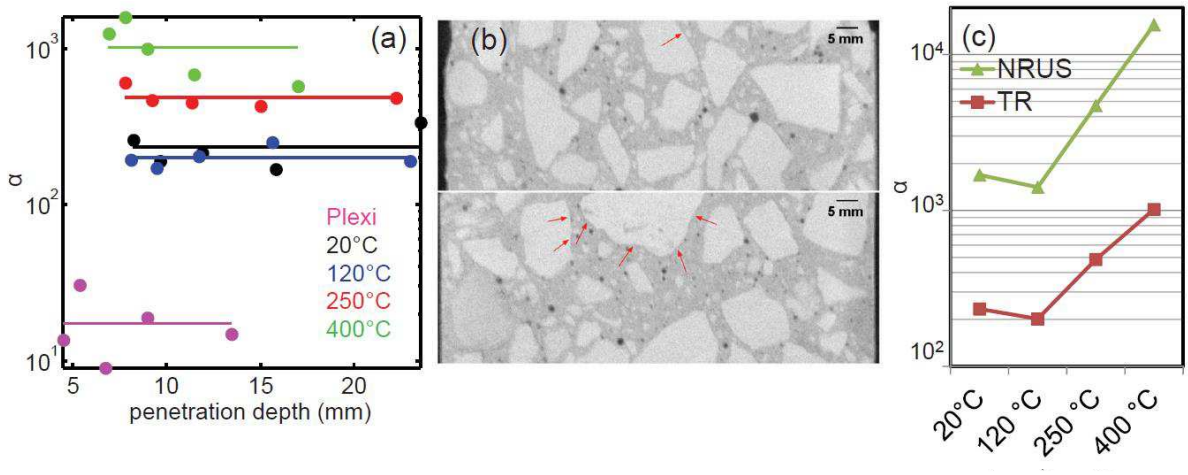

FIG. 2. (Color online) (a) Compilation of the results. Solid lines are the average nonlinearity for each sample. (b) Xray CT images of the 20°C sample (top) and the 400°C sample (bottom). (c) Comparison of the average nonlinearity noted TR with NRUS data from [8].

We show in this letter the feasibility of using time reversal at various frequencies to probe the nonlinearity of materials at various depths. The correlation of the results with reference measurements from the literature, along with X-ray CT images which explain the results for the 400°C sample, validates the concept. The time delay observed in the experiments, a signature of nonlinear mesoscopic elasticity, suggests a physically based method to quantitatively evaluate the nonlinearity. This approach could be extended to the classical nonlinearity by monitoring the harmonic content with increasing amplitude or slow dynamics by looking at the slow recovery of initial focal time. A better estimation of strain amplitude is under study by further numerical simulations associated with three component laser measurements. It should ultimately allow precise and local nonlinearity measurements using a time reversal mirror and it has the potential to be easily applied *in situ* for practical applications, such as inspection of concrete infrastructures.

Acknowledgments

Authors thank the US DOE Used Fuel Disposition (Storage) campaign and the Electrical Power Research Institute for supporting this study and Payan's visit to LANL. Payan was also supported by Aix Marseille Univ. We would also like to thank James Ten Cate, Paul Johnson, and Robert Guyer for useful discussion during the course of this work.

References

1 C. Draeger, J.C. Aime, and M. Fink, *J. Acoust. Soc. Am.* 105(2), 618 (1999).

2 M. Fink, *IEEE Trans. Ultrason. Ferroelectr. Freq. Control.* 39(5), 555 (1992).

3 T.J. Ulrich, P. A. Johnson, and Guyer, R. A., *Phys. Rev. Lett.* 98, 104301 (2007).

4 T.J. Ulrich, A. Sutin, T. Claytor, P. Papin, P.Y. Le Bas, and J.A. TenCate,, *App. Phys. Lett.* 93, 151914 (2008).

5 P.Y. Le Bas, T.J. Ulrich, B.E. Anderson, R.A. Guyer, and P.A. Johnson, *J. Acoust. Soc. Am.* 130(4), EL258 (2011).

6 E. Janssen E., K. Van Den Abeele, *Ultrasonics* 51(8), 1036 (2011).

7 M. Scalerandi, A.S. Gliozzi, C.L.E. Bruno and K. Van Den Abeele, *J. Phys. D: Appl. Phys.* 41, 215404 (2008).

8 C. Payan, T.J. Ulrich, P.Y. Le Bas, T.A. Saleh, M. Guimaraes, *J. Acoust. Soc. Am.* (Revision sent, 2014).

9 A. Derode, P. Roux, M. Fink, *Phys. Rev. Lett.* 75, 4206 (1995).

10 R. Guyer and P.A. Johnson, *Nonlinear Mescopic Elasticity* (Wiley-VCH Ed., Berlin, 2009).

11 J. Rivière, S. Haupert, P. Laugier, P.A. Johnson, *J. Acoust. Soc. Am.* 132(3), EL202 (2012).

12 V. Tournat and V. E. Gusev, *Phys. Rev. E* 80(1), 011306 (2009).

13 J.A. TenCate, D. Pasqualini, S. Habib, K. Heitmann, D. Higdon, and P.A. Johnson, *Phys. Rev. Lett.* 93(6), 065501 (2004).

14 M. Scalerandi, A.S. Gliozzi, C.L.E. Bruno, P. Antonaci, *Phys. Rev. B* 81, 104114 (2010)

15 See supplemental material at […] for details about X-ray tomography measurements.

16 M. Scalerandi, M. Griffa, P. Antonaci, M. Wyrzykowski and P. Lura, *J. Appl. Phys.* 113, 154902 (2013).

17 J. Bisschop and J.G.M. van Mier, *Mat. Struct.* 35, 453 (2002).